

# Analytical Model for Magnetic Anisotropy Dedicated to Non-Oriented Steel Sheets

Floran Martin, Deepak Singh, Anouar Belahcen, Paavo Rasilo, Ari Haavisto, and Antero Arkkio

Aalto University - Department of Electrical Engineering and Automation, Otakaari 5, 02150 Espoo, Finland  
E-mail: floran.martin@aalto.fi

**Abstract**—Recent investigations on magnetic properties of Non-Oriented steel sheets enhance the comprehension of the magnetic anisotropy behavior of widely employed electrical sheets. Our investigation consists of developing an analytical model to consider these magnetic properties while modelling electromagnetic systems. From rotational measurements, the anhysteretic curves are interpolated in order to extract the magnetic energy density for different directions and amplitudes of the magnetic flux density. Furthermore, the analytical representation of this energy is suggested based on statistical distribution which aims to minimize the intrinsic energy of the material. Our model is finally validated by comparing measured and computed values of the magnetic field strength.

**Index Terms**—Magnetic properties, Non-Oriented steel sheets, Anisotropy

## I. INTRODUCTION

Non-oriented (NO) electrical steel sheets are usually composed of iron doped with silicon. Although their manufacturing process tends to confer isotropic properties [1], [2], magnetic anisotropy has been always observed and recently investigated [3], [4], [5]. Three main intrinsic phenomena involve anisotropic characterization of body centered cubic iron [6]:

- *Shape anisotropy* is a purely magnetostatic phenomenon. It depends on the shape of ferromagnetic crystal and its magnetic moment. These magnetic moments within the crystal produce not only an external magnetic field but also an internal field known as the demagnetization field [7].
- *Magnetocrystalline anisotropy* is mainly caused by spin-orbit interaction [8]. Thus it depends on the molecular structure of the crystal. In grain-oriented (GO) electrical steel sheet, the body centered cubic structure for pure iron is enhanced in order to bring a hard direction in the diagonal of the cube. With NO steel sheet, this phenomenon is diminished.
- *Magnetostriction* results by strain due to an external field which rotates magnetic moments [8]. Although, this effect would be neglected in case of perfectly spheroidal crystal, the spin-orbit interaction also involves significant magnetomechanical effects on electrical sheets (vibration, additional losses, ...) [9], [8], [10], [11].

Models of magnetic anisotropy derive from different formulations regarding to the target application. The following non-exhaustive literature review considers applications dedicated to finite element formulation. Since the magnetic anisotropy infers a dependance of reluctivity on both amplitude and direction of the applied flux density, its model can be developed by interpolating between two adjacent measured  $\mathbf{B} - \mathbf{H}$  curves [12]. Under rotational applied flux density, Enokizono and Soda [13] develop a Garlérkin's formulation based on the decomposition of the magnetic field into a

purely rotational field (isotropic) and an effective field (anisotropic). The isotropic reluctivity and components of the effective magnetic field are interpolated and implemented into their numerical method.

Derived from magnetocrystalline theory [9], Vernescu-Spornic et al. [14] develop a mixed Preisach/biastruide model. The biaxial anisotropy is considered by minimizing the sum of the applied field and the magnetocrystalline anisotropy energy, which depends on the first anisotropy constant. Their model was validated by comparison with measurements on NiFe samples at 1.5 T and 50 Hz under rotating induction, alternating sinusoidal along hard direction and both rolling and transverse directions. However discrepancies were noticed at low flux level especially under rotational measurements. Considering the phase mode theory [15], Fiorillo et al. [16] investigate the impact of experimental setup on magnetic measurements of GO iron steel sheets under alternating flux. Their improved model includes not only the first and the second anisotropy constants but also hysteresis loops. From 0.4 to 1.5 T, their model fits well with measurements performed on X-stack (low effect of shape anisotropy), Epstein frame and Single Sheet Tester.

Based on energy/coenergy density principle [17], Péra et al [18], [19] expand a phenomenological model on GO sheets which needs only the rolling (RD) and the transverse (TD) direction given by manufacturers. For low value of coenergy density (shape anisotropy), hard direction is close to  $90^\circ$  while the hard direction appears, in theory, in the diagonal of a cubic crystal ( $55^\circ$ ) for higher coenergy density level. Although, their computational implementation requires some numerical derivation based on interpolation, their model matches with alternating flux measurements for 4 various directions in the range of 200 A/m to 30 kA/m. However, the four magnetization modes introduced by Néel [15]

are not fully described by this phenomenological approach, so data in more directions are needed to characterize these sheets completely [4], [20]. Thus, Higuchi et al. [4] model the magnetic energy density for NO sheets with Fourier series. Their decomposition is based on alternating flux with 7 different cutting angles on Single Sheet Tester [21]. Their approach shows that magnetic anisotropy impacts on torque ripples and hysteresis losses of an interior permanent magnet motor.

In this paper, we present an original model developed by including Gumbel distribution on energy density principle. Originally, Gumbel distribution can be employed to model the distribution of the maximum (or the minimum) corresponding to many samples characterized with various distributions [22]. The arrangement of the grains, containing different crystals within the sheets, depends on manufacturing process. Grain size, wall thickness, and magnetic moment orientation differ within the NO sheets. While applying an external field, we assume that this macroscopic structure will move in order to minimize its intrinsic energy. As energy density is a scalar, its implementation in finite element method should result in faster resolution of the energy functional formulation than manipulating  $\mathbf{B}$  and  $\mathbf{H}$  vectors. Whereas the energy density presents an implicit form in [18], [23], we suggest an explicit formulation in order to ease the computations. The proposed model is fitted with 16 parameters from 9 rotational measurements with Gumbel functions.

## II. EXTRACTION OF ENERGY DENSITY FROM ROTATIONAL MEASUREMENTS

Measurements have been carried out in two cross shape NO sheets [24]. In order to reduce the effect of shape anisotropy [16], the rolling direction of both sheets are shifted by  $180^\circ$ . Every component of  $\mathbf{B} - \mathbf{H}$  loci are measured with 3 072 points at 10 Hz. Rotating magnetic flux density presents 9 different amplitudes: 0.2 T, 0.42 T, 0.64 T, 0.87 T, 1.09 T, 1.34 T, 1.52 T, 1.65 T, and 1.89 T. We are interested in extracting the anisotropic energy density which does not produce losses over a cycle.

### A. Interpolation of anhysteretic curves

In order to retrieve the anhysteretic curves, we remove the hysteresis by assuming that  $\mathbf{B}$  loci are perfectly circular. Along each locus, hysteresis induces an average phase difference  $\phi_{hys}$  between the magnetic flux density and the magnetic field strength over a full cycle. Hence, components  $h_x$  and  $h_y$  are calculated by :

$$\begin{bmatrix} h_x \\ h_y \end{bmatrix} = \begin{bmatrix} \cos \phi_{hys} & \sin \phi_{hys} \\ -\sin \phi_{hys} & \cos \phi_{hys} \end{bmatrix} \times \begin{bmatrix} h_{x-meas} \\ h_{y-meas} \end{bmatrix} \quad (1)$$

where  $h_{x-meas}$  and  $h_{y-meas}$  correspond to measured magnetic field strength components.

Since the anisotropic angle between magnetic magnitude presents less variation when the material approaches its saturation, the reference angle  $\phi_{h-max}$  corresponds to the  $\mathbf{H}$  locus matching with 1.89 T  $\mathbf{B}$  locus. From the 3 072 different directions, we select the amplitude of 9  $\mathbf{H}$  loci whose polar angle is closest to the reference. While each  $\mathbf{H}$  amplitude is associated with its corresponding  $\mathbf{B}$  amplitude,  $H(B)$  anhysteretic curves (Fig. 1) are extracted and interpolated with a shape-preserving piecewise cubic polynomial function.

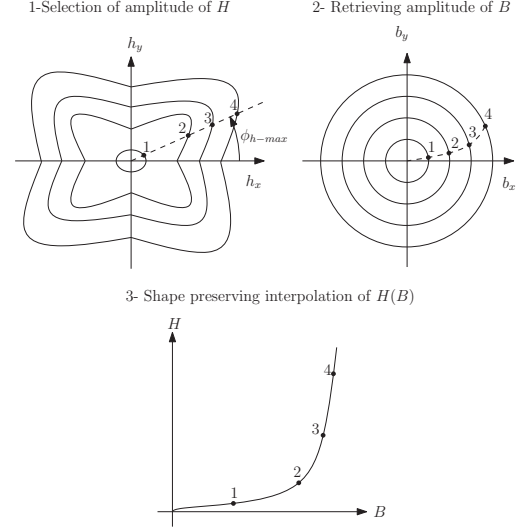


Fig. 1: Representation of the method for determining the anhysteretic curves from  $\mathbf{B} - \mathbf{H}$  loci for a given direction  $\phi_{h-max}$

### B. Energy density distribution and equal contour of energy density

The energy density  $w(b_x, b_y)$  is computed by integration of the interpolated anhysteretic curves by :

$$w(b_x, b_y) = \int_0^{\mathbf{B}} \mathbf{H} \cdot d\mathbf{B} \quad (2)$$

Figure 2 represents the extracted energy density from the measurements by the described method.

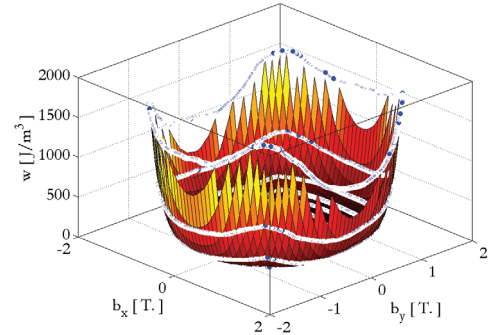


Fig. 2: Representation of the magnetic energy density  $w(b_x, b_y)$  extracted from the quasi-static measurements

This energy density is interpolated by a surface spline in order to compute equal contour of energy density. From the 0.2 T and 1.89 T loci, the highest and the lowest energy density are respectively selected for both extrema contours of energy density. With all other loci, average values of energy density are retained in order to compute the equal contour of energy with Brent's method [25]. Figure 3 represents the equal contours of energy density.

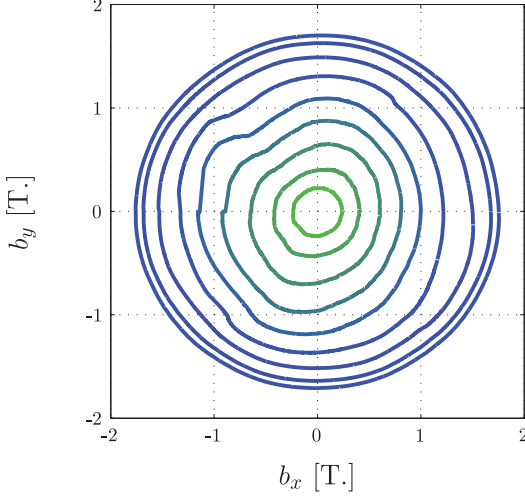


Fig. 3: Contours of equal energy corresponding to the interpolated anhysteretic curves

Since, we aim to improve the modified elliptic model of isolines of energy developed by T. Péra et al. [18], [23], we compute the value of energy density  $w_0$ , the intersection  $B_{x0}$  and  $B_{y0}$  between these contours and both axes  $(0, b_x)$  and  $(0, b_y)$  respectively, and the parameter  $n$  which is equal to 2 in the specific case of elliptic contours (Tab. I).

TABLE I: Data of equal energy contours

$w_0$ [J/m <sup>3</sup> ]	$B_{x0}$ [T]	$B_{y0}$ [T]	$n$
5.55	0.238	0.2249	2.098
13.3	0.408	0.3977	2.362
24.4	0.606	0.6494	2.348
38.3	0.8107	0.8698	2.200
56.8	1.000	1.0878	2.028
96.6	1.2178	1.3062	2.092
231	1.500	1.4898	2.000
621	1.6792	1.6272	2.000
1053	1.7541	1.7012	2.011

### III. ANALYTICAL REPRESENTATION BASED ON GUMBEL DISTRIBUTION

The modified elliptic model represents the equal contour of energy density with the following assumptions [18], [23]:

- $\mathbf{B}$  and  $\mathbf{H}$  are collinear in both rolling and transverse directions so equal contours of energy density are orthogonal to these directions;
- Hysteresis is neglected in order to provide a monotonous implicit function  $H_y(H_x)$ ;

Thus equal contours of energy density can be modeled by the following implicit function  $F$ :

$$F(b_x, b_y) = \left(\frac{b_x}{B_{x0}}\right)^n + \left(\frac{b_y}{B_{y0}}\right)^n - 1 = 0 \quad (3)$$

The 3 functions  $B_{x0}$ ,  $B_{y0}$ , and  $n$  can also be calculated as a function of the energy density as in [18], [23].

#### A. An improved expression of energy density

With our approach, we propose an explicit expression of the energy density in order to compute components of magnetic field by analytical differentiation. In its general form, energy density could be expressed by :

$$w(b_x, b_y) = C(b_x, b_y) b_x^{n(b_x, b_y)} + D(b_x, b_y) b_y^{n(b_x, b_y)} \quad (4)$$

Where  $C$ ,  $D$ , and  $n$  are 3 functions that only depend on the components of magnetic flux density.

With the suggested model, equal contours of energy density are linked with the original approach by :

$$F = \frac{C}{w_0} b_x^n + \frac{D}{w_0} b_y^n - 1 \quad (5)$$

By simple identification of (5) and (3), we can notice that functions  $n$  are the same and functions  $C$ ,  $D$  can be computed by :

$$\begin{aligned} C &= \frac{w_0}{B_{x0}^n} \\ D &= \frac{w_0}{B_{y0}^n} \end{aligned} \quad (6)$$

These 3 functional parameters can be interpolated by piecewise polynomials but in order to ease the computation of energy density differentiations, we suggest an interpolation by Gumbel distributions.

#### B. Representation and interpolation of functional parameters

Considering NO steels, functions  $C$ ,  $D$ , and  $n$  can be expressed as a function of the amplitude of magnetic flux density  $B$ . Originally, Gumbel distribution aims to approach the maximum value corresponding to many samples with different distributions. While applying an external field, we assume that grains and walls will move in order to minimize the intrinsic energy. Hence, functional parameters  $C$  and  $D$  could be interpolated with the inverse of a Gumbel function  $g$ . The functional parameters  $n$  which corresponds to the intrinsic magnetic moment could be modeled with a Gumbel function too. Moreover, from the extracted value of  $n$  (Tab. I), we can

notice that the elliptic assumption would be correct in both cases : without applied field and when steel reaches its saturation. So, we suggest the following interpolated functions :

$$C(B) = g(B, \alpha_C, b_C, \beta_C, k_C)^{-1}$$

$$D(B) = g(B, \alpha_D, b_D, \beta_D, k_D)^{-1} \quad (7)$$

$$n(B) = g(B, \alpha_C, b_C, \beta_C, k_C) + 2$$

Where  $B$  is the amplitude of the magnetic flux density,  $\alpha$ ,  $b$ ,  $\beta$ , and  $k$  are the parameters of the Gumbel distribution. The Gumbel distribution is given by:

$$g(B) = \alpha \exp \left[ -\frac{B-b}{\beta} - \exp \left( -\frac{B-b}{k\beta} \right) \right] \quad (8)$$

The functional parameters  $C$ ,  $D$ , and  $n$  are represented in figures 4-6.

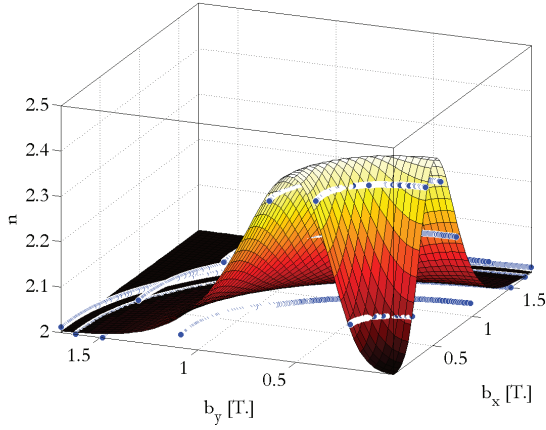


Fig. 4: Representation of the function  $n(b_x, b_y)$  fitted by the contour of equal energy

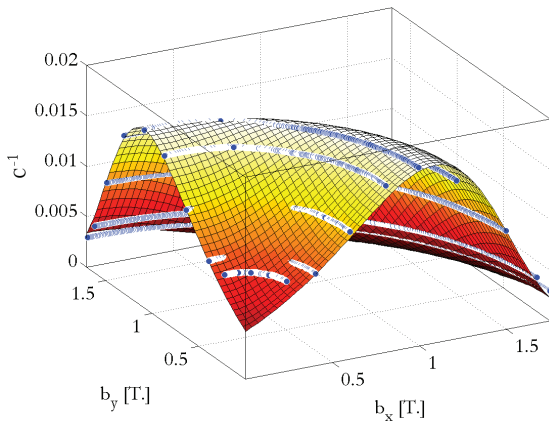


Fig. 5: Representation of the function  $1/C(b_x, b_y)$  fitted by Gumbel distribution

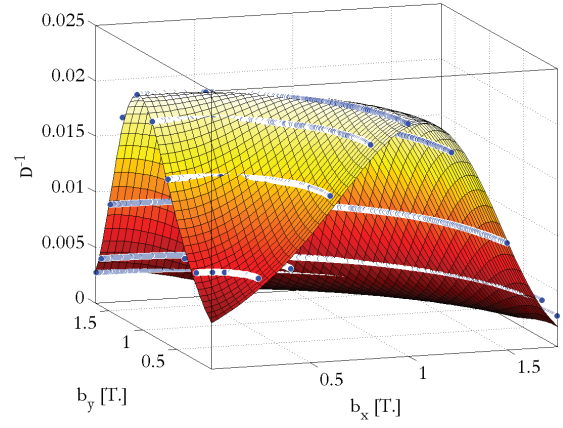


Fig. 6: Representation of the function  $1/D(b_x, b_y)$  fitted by Gumbel distribution

The fitted parameters, error and correlation coefficients are given in table II.

TABLE II: Parameters of the Gumbel distributions to model  $n$ ,  $C$ , and  $D$  in the energy density model

	$n(b_x, b_y)$	$C^{-1}(b_x, b_y)$	$D^{-1}(b_x, b_y)$
$\alpha$	1.041	0.0456	0.0569
$b$	0.6135	1.2209	1.0568
$\beta$	0.1856	-0.5473	-0.4140
$k$	1.3809	0.7054	1.0378
Correlation $r^2$	0.9979	0.9749	0.9834
Error $rmse$	0.0063	0.0007	0.0008

First, we can notice that Gumbel distribution provides both good correlation coefficients and small root mean square errors for the interpolation of the 3 functional parameters  $C$ ,  $D$ , and  $n$ . Then, parameter  $k$  which is originally equal to 1 is close to unity. Since we model  $C$ ,  $D$ , and  $n$  to describe the energy density as a function of the amplitude of  $\mathbf{B}$ , we suppose that equal contours of energy are close to elliptic shape. The parameter  $k$  which allows a modification of original slopes of Gumbel distribution, has been introduced in order to overcome this assumption and improve the interpolation.

#### IV. INVESTIGATION ON THE SUGGESTED MODEL

The  $\mathbf{H}$  loci can be determined by differentiating the energy density with respect to the components of flux density. These computed  $\mathbf{H}$  loci are compared with the measured loci. A sensitivity analysis is introduced to evaluate the effect of uncertainty on flux density measurements.



### A. Comparison between measured and computed magnetic field

Components of magnetic field strength are determined by:

$$h_x = \frac{\partial w(b_x, b_y)}{\partial b_x} \quad (9)$$

$$h_y = \frac{\partial w(b_x, b_y)}{\partial b_y}$$

These components only depend on the components of magnetic flux density and parameters of Gumbel distribution. Hence,  $\mathbf{H}$  loci can be computed from measured  $\mathbf{B}$  loci. In figures 7a-7i, we can notice that both measured and computed  $\mathbf{H}$  loci present similar shapes. For higher value of magnetic flux density, the flower shape related to anisotropy is reproduced by the suggested model and for low value of magnetic flux density, the model reproduces a quasi-isotropic shape. Then, the average relative error between the model and the measurements is 27 %. The highest error is reached for the locus corresponding to the amplitude of 1.79 T of magnetic flux density (Fig. 7i). Therefore, we propose to investigate the impact of errors in the measurements of the magnetic flux density.

### B. A sensitivity analysis

In order to appreciate the comparison between computed and measured  $\mathbf{H}$  loci, we propose to modeled  $\mathbf{H}$  loci with an error of  $\pm 5\%$  on the measurements of  $b_x$  and  $b_y$ . The gray area in figure 7a-7i represent the impact of this error on the computed magnetic field strength. We can notice that for 1.79 T which contains the maximum error of our proposed model, the impact of uncertainty in magnetic flux density measurements is strongly significant. Thus, it may not be relevant to estimate the accuracy of the model based on this locus. Besides, since the  $\mathbf{B}$  loci are not perfectly circular, their hysteresis angles differ within every locus. Hence, the proposed method to extract the  $B - H$  anhysteretic curves for different directions also presents some error. Although, errors arise from different phenomena, the proposed method models the magnetic anisotropy of non-oriented steel sheets with relatively low error (27 %).

## V. CONCLUSION

The proposed model is based on an analytical formulation of the energy depending on the components of the magnetic flux density. This formulation is composed of 3 Gumbel distributions. Every functional parameters of energy density is formulated with only 4 parameters which are calculated by fitting the energy extracted from measurements. The components of the magnetic field are then deduced by differentiating the magnetic energy with respect to the components of the magnetic flux density. Hence, with this analytical formulation, the determination of  $\mathbf{H}$  does not require

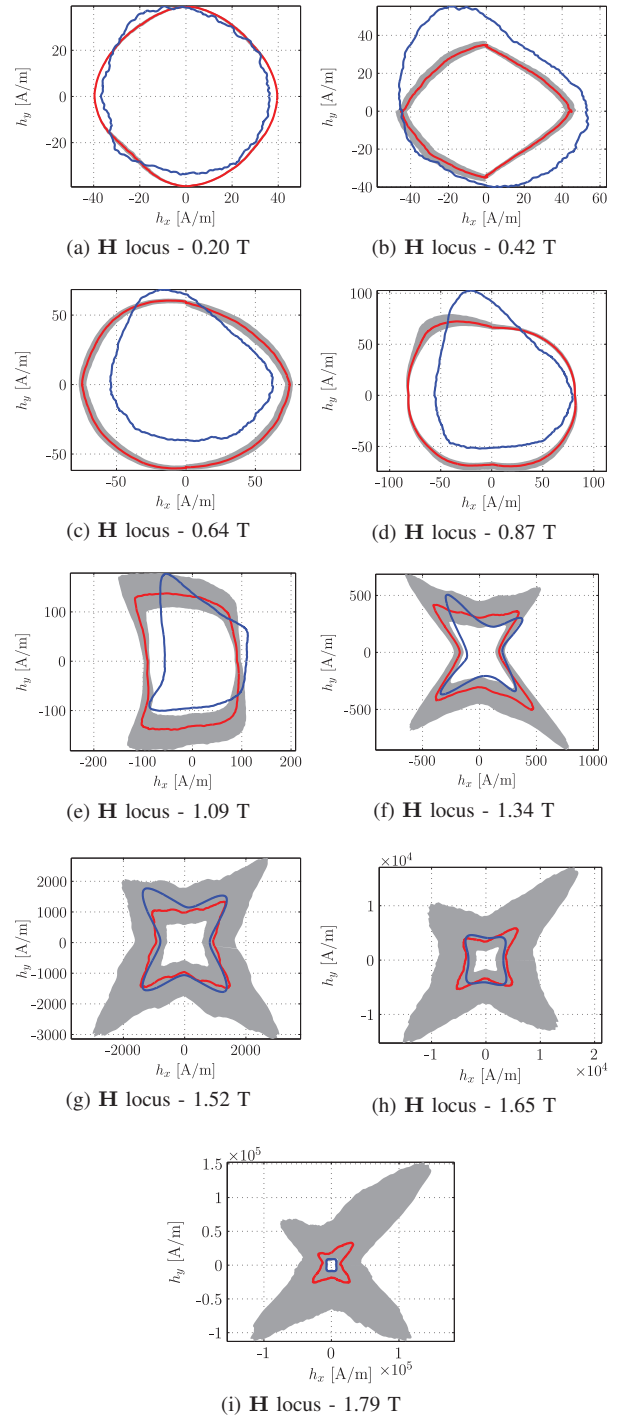


Fig. 7: Comparison of the calculated magnetic field (in red) and the measured field (in blue) from the rotating measure at 10 Hz. The grey area corresponds to the impact of  $\pm 5\%$  of error in flux density measurements on the computed field.

any iterative process as it is usually the case with this energy method coupled with implicit function. Finally, the proposed model is validated by comparing the computation and the measurements of 9  $\mathbf{H}$  loci for non-oriented steel sheets at 10 Hz. The proposed analytical

model shows good agreements with an average relative error of 27 %.

In further work, it could be relevant to improve the measurement control in order to apply perfectly circular loci of the rotating flux density. Besides, implementation of the proposed model in 2D finite element method is actually in process in order to highlight the effectiveness and usefulness of the suggested method.

#### REFERENCES

- [1] A. Kedous-Lebouc, *Matériaux magnétiques en génie électrique 1*. Paris: Lavoisier, hermès sciences ed., 2006.
- [2] P. Rasilo, E. Dlala, K. Fonteyn, J. Pippuri, A. Belahcen, and A. Arkkio, "Model of laminated ferromagnetic cores for loss prediction in electrical machines," *Electric Power Applications, IET*, vol. 5, pp. 580–588, August 2011.
- [3] K. Chwastek, "Anisotropic properties of non-oriented steel sheets," *Electric Power Applications, IET*, vol. 7, pp. 575–579, Aug 2013.
- [4] S. Higuchi, Y. Takahashi, T. Tokumasu, and K. Fujiwara, "Comparison between modeling methods of 2-d magnetic properties in magnetic field analysis of synchronous machines," *Magnetics, IEEE Transactions on*, vol. 50, pp. 373–376, Feb 2014.
- [5] P. Handgruber, A. Stermecki, O. Bíró, V. Goričan, E. Dlala, and G. Ofner, "Anisotropic generalization of vector preisach hysteresis models for non-oriented steels," in *Conference on Electromagnetic Field Computation - CEFC*, (Annecy), 2014.
- [6] S. Chikazumi, *Physics of Ferromagnetism*. Oxford University Press, 1997.
- [7] J. Osborn, "Demagnetizing factors of general ellipsoid," *Phys. Rev.*, vol. 67, pp. 351–357, 1945.
- [8] B. D. Cullity and C. D. Graham, *Introduction to Magnetic Materials, 2nd Edition*. Wiley-IEEE Press, 2008.
- [9] R. Skomski, *Simple Models of Magnetism*. Oxford University Press, 2008.
- [10] A. Belahcen, D. Singh, P. Rasilo, F. Martin, S. Ghalamestani, and L. Vandervelde, "Anisotropic and strain-dependent model of magnetostriction in electrical steel sheets," in *CEFC*, (Annecy), XVI Conference on Electromagnetic Field Computation, 2014.
- [11] K. Fujisaki, Y. Nemeto, and R. Hirayama, "Electromagnetic steel solution in electromagnetic field technique," Tech. Rep. 89, Nippon Steel Technical Report, 2004.
- [12] G. Shirkoohi and J. Liu, "A finite element method for modelling of anisotropic grain-oriented steels," *IEEE Trans. On Magnetics*, vol. 30, no. 2, pp. 1078–1080, 1994.
- [13] M. Enokizono and N. Soda, "Magnetic field analysis by finite element method using effective anisotropic field," *IEEE Trans. On Magnetics*, vol. 31, no. 3, pp. 1793–1796, 1995.
- [14] C. Vernescu-Spornic, A. Kedous-Lebouc, S. A. Spornic, and F. Ossart, "Anisotropic and vector hysteresis model for magnetic materials application to a cubic textured nife sheet," *Physica B: Condensed Matter*, vol. 275, no. 13, pp. 99 – 102, 2000.
- [15] L. Néel, "Les lois de l'aimantation et de la subdivision en domaines élémentaires d'un monocristal de fer," *J. Phys. et Radium*, vol. 5, no. 11, pp. 241–251, 1944.
- [16] F. Fiorillo, R. Dupré, C. Appino, and A. M. Rietto, "Comprehensive model of magnetization curve hysteresis loops, and losses in any direction in grain-oriented fe-si," *IEEE Trans. Magn.*, vol. 38, no. 3, pp. 1467–1476, 2002.
- [17] P. P. Silvester and R. P. Gupta, "Effective computational models for anisotropic soft b-h curves," *IEEE Trans. On Magnetics*, vol. 27, no. 5, pp. 3804–3807, 1991.
- [18] T. Péra, F. Ossart, and T. Waeckerle, "Field computation in non linear anisotropic sheets using coenergy model," *IEEE Trans. On Magn.*, vol. 29, no. 6, pp. 2425–2427, 1993.
- [19] T. Péra, F. Ossart, and T. Waeckerle, "Numerical representing for anisotropic materials based on coenergy modeling," *J. Appl. Phys.*, vol. 73, no. 10, pp. 6784–6786, 1993.
- [20] G. Meunier, *The Finite Element Method for Electromagnetic Modeling*. Wiley-ISTE, 2008.
- [21] S. Higuchi, T. Nakao, Y. Takahashi, T. Tokumasu, K. Fujiwara, and Y. Ishihara, "Modeling of two-dimensional magnetic properties based on one-dimensional magnetic measurements," *Magnetics, IEEE Transactions on*, vol. 48, pp. 3486–3489, Nov 2012.
- [22] E. Gumbel *Ann. Inst. Henri Poincaré*, vol. 5, no. 2, pp. 115–158, 1935.
- [23] O. Bíró, S. Außerhofer, K. Preis, and Y. Chen, "A modified elliptic model of anisotropy in nonlinear magnetic materials," *Compel*, vol. 29, no. 6, pp. 1482–1492, 2010.
- [24] M. Belkasim, "Identification of loss models from measurements of the magnetic properties of electrical steel sheets," Master's thesis, Helsinki University of Technology, 2008.
- [25] R. Brent, *Algorithms for Minimization without Derivatives*. Prentice-Hall, 1973.